

## ***Interactive comment on “Atmospheric winter conditions 2007/08 over the Arctic Ocean based on NP-35 data and regional model simulations” by M. Mielke et al.***

**M. Mielke et al.**

Klaus.Dethloff@awi.de

Received and published: 13 August 2014

Answers to anonymous referee 2

Atmospheric winter conditions 2007/08 over the Arctic Ocean based on NP-35 data and regional model simulations by Mielke et al.

We thank the reviewer for careful reading the manuscript and useful comments.

1. Model runs A regional climate model (RCM) generates from lower-resolution lateral boundary conditions, dynamically consistent high resolution atmospheric fields. Laprise (2008) showed in ensemble simulations with a RCM, that beside the forced  
C5862

component as a result of prescribed sea-surface and lateral boundary conditions, departures from the ensemble mean, the so called free component appears on spatial scales below 1100 km due to internally generated variability. In this way, RCMs are capable of generating regional and meso-scale features absent in the driving fields. This is the added value of the presented HIRHAM simulations on climate time scales. We believe therefore, that the comparison of forecast mode and climate model simulations against single station data makes sense, although the assessment of regional model quality is an unsolved issue. Laprise, R., 2008, Challenging some tenets of Regional Climate Modelling, Meteorol. Atmos. Phys., 100, 3–22, DOI 10.1007/s00703-008-0292-9

On monthly time scales the atmospheric model in climate mode forget about the initial state, but the different initial states interact with the lateral boundary conditions and induce different free components on spatial scales below 1100 km. In a large integration area during continuous integrations over the whole winter a phase state divergence with a decoupling of the lateral forcing from the interior solution can occur. This can be partly avoided by monthly reinitialisations as done in our model simulations. Another way would be to apply nudging techniques as suggested by von Storch et al. (2008). Von Storch, H., H. Langenberg, and F. Feser, 2000, A spectral nudging technique for dynamical downscaling purposes, Mon. Wea. Rev., 128, 3664-3674.

Page 11868, LN 13-18: Here we changed the text to: “The HIRHAM clima run is the only ensemble member which reproduces the two distinct circulation states shown in Fig. 10. All other ensemble members with the same initialization as HIRHAM clima are not able to reproduce the two local maxima in the frequency distribution of net LW. The HIRHAM b10 run with the same initialization as HIRHAM clima indicates a weaker second maximum.”

2. Use of monthly means/synoptic situations We computed the atmospheric temperature profiles for the two different surface net long wave radiation conditions and describe the results in the new Figure 10 b. These profiles and further results described

in the additional Fig. 16 indicate that the Arctic atmosphere is a complex system with nonlinear interactions and complex feedbacks between planetary and baroclinic circulation systems and temperature and cloud cover changes in the lower atmosphere and Arctic PBL.

New Fig. 10 b. Vertical temperature (K) and relative humidity (%) profiles for a) net LW circulation state below  $30 \text{ Wm}^{-2}$  and b) net LW circulation state above  $30 \text{ Wm}^{-2}$  averaged over NDJFM. The results are described in the text as follows. "The two radiative circulation states differ in their vertical structure. The net LW radiation state above  $30 \text{ Wm}^{-2}$ , connected with higher pressure is drier and colder (ca 3 K at 900 hPa) than the state below  $30 \text{ Wm}^{-2}$ ."

3. Explanation of model biases Our sensitivity experiments using different stability functions emphasize the importance of nonlinear interactions between the Arctic PBL, synoptical and planetary scales with the potential to induce changes in the vertical feedbacks of the PBL column with respect to surface energy budget, vertical fluxes and clouds.

We recomputed the Figs. 13-15 by including the HIRHAM f12 simulations and computed area averaged results (rectangles indicated by white lines in Figs. 13-15) in the new Fig. 16. Exemplarily we show here the newly computed Fig. 14.

This has been described in the text in the following way: "The increased vertical stability in the model simulations does not show an influence on synoptical time scales 1-3 days, but leads to reduced planetary-scale variability on time scales of 2-10 and 10-20 days in all winter months."

New Fig. 14. Pan-Arctic distribution of baroclinic-scale variability on time scales from 2–10 days expressed as filtered temporal standard deviation of 6 hourly mean sea level pressure (hPa) for November 2007 (upper row) until March 2008 (lower row) and December, January and February in between. From left to right ECMWF operational analyses, HIRHAM f12 simulations, HIRHAM clima simulations with  $b = 5$ , and

C5864

HIRHAM b10 with  $b = 10$ .

New Fig. 16. Area mean (rectangle indicated by white lines in new Figs. 13-15) of the synoptic and planetary-scale variability on time scales 1-3 days, 2-10 days and 10-20 days for December 2007 (left), January (middle) and February 2008 (right). The results are based on filtered standard deviation of 6 hourly mean sea level pressure (hPa). Red column-ECMWF, Grey column-HIRHAM f12, Green column-HIRHAM clima with  $b5$ , Blue column-HIRHAM  $b10$ .

With respect to the suggestion of the impact of surface conditions we added the following sentence on page 11864, LN 9: A reduction of sea ice thickness from 2m to 1m reduces the temperature correlation coefficient between model simulations and the NP-35 observations at 1000 hPa from 0.58 to 0.55 and at 500 hPa from 0.74 to 0.66.

On P11869, L20 we added: Turbulent mixing is determined by the surface roughness, the thermal stratification and the vertical wind shear.

4. Clarity of presentation We deliver the requested information in the text.

Relative humidity is always w.r.t. ice.

Fig. 7 is based on 12 hourly NP-35 data and 6 hourly model output.

To count inversions, we applied the definition of Kahl (1990), which we cite now in the manuscript. The inversion height is the depth of the inversion. Kahl, J. D., 1990, Characteristics of the low-level temperature inversion along the Alaskan Arctic coast, *Int. J. Climatol.*, 10, 537-548. The wind speed in the LLJ maximum has to exceed the threshold value of 12 m/s and a minimal wind speed gradient of 8 m/s in the range from the surface to the height of LLJ.

Specific comments:

5. We changed this to: The impact of internal atmospheric dynamics on the ...

6. We cite the paper Persson et al. (2002) in the introduction on page 11857, LN 13.

C5865

Persson, P. Ola G., C. W. Fairall, E. L. Andreas, P. S. Guest, and D. K. Perovich, 2002: Measurements near the Atmospheric Surface Flux Group tower at SHEBA: Near-surface conditions and surface energy budget. *J. Geophys. Res.*, 107, C10, 8045, doi:10.1029/2000JC000705.

7. On pp 11859-11860 we changed from past perfect to perfect.

8. P 11861, L1: These roughness lengths are used over the sea ice covered ocean. Over land the roughness length is a function of subgrid-scale orography and vegetation.

9. On page 11861, L 8 we changed the sentence to: A value of  $b=10$  was applied in selected sensitivity experiments for more stable stratification, where the stability functions decrease more strongly with increasing stability.

10. On page 11861, L10 we changed to: Above the surface layer a 1.5 order closure scheme was applied. . .

11. There is no snow layer on sea ice in this model setup.

12. On P 11862 L 1 we introduced the sentence: The HIRHAM b10 setup is the same as for HIRHAM clima, but instead of  $b=5$  for HIRHAM clima a value of  $b=10$  is used. The comparison between HIRHAM clima and HIRHAM b10 with respect to the vertical profiles is shown in Fig. 6. We computed additionally the new Fig. 10 b, where we compare the vertical temperature profiles for the two different surface net LW radiation states. The results are described in the text as follows. "The two radiative circulation states differ in their vertical structure. The net LW radiation state above  $30 \text{ Wm}^{-2}$  is drier and colder (ca 3 K at 900 hPa) than the state below  $30 \text{ Wm}^{-2}$ ."

13. On P 11862, L8 we introduced the sentence: The forecast model is initialized every 12 hours at 00.00 UTC and 12.00 UTC.

14. On P 11864 we added the following sentences: The colours describe the local wavelet power normalized by  $1/(\sigma \times \sigma)$  in the different frequency bands. The edge effects are due to finite-length time series.

C5866

15. On page 11866, L19 we changed the sentence to: The surface inversion strength in the lower troposphere differs considerably.

16. On page 11866, L11 we introduced the following sentences: During the months with very low temperatures December, January and February the HIRHAM clima and the HIRHAM b10 runs differ remarkably. In these months the enhanced vertical stability leads to lower temperatures throughout the whole troposphere. Especially in January the HIRHAM b10 fits the observations better.

17. On P11866, L12 we changed the sentence to: Based on Fig. 6, the across-ensemble scatter simulations for temperature, wind speed and relative humidity, described by the  $\pm 1$  standard deviations in the HIRHAM ens varies during the winter.

18. On Page 11867, L 8 we changed the sentence to: Figure 9 compares the frequency of temperature inversions at the surface and at different heights and their strengths for November 2007-March 2008 from the measurements and the HIRHAM simulations. Correspondingly we changed the description of Fig. 9 to: Frequency of occurrence of temperature inversion heights between the surface and 1460 m (a), and of strength of vertical temperature inversion (b) for NP-35 radiosondes (green) and model simulations HIRHAM ens (black) and HIRHAM f12 (red) at NP-35 location.

19. On page 11868 we wrote an explanation as follows: The HIRHAMf12 simulations apply a nudging to the operational ECMWF analyses every 12 hours and it seems that beside the accurate initial states internally generated variability on monthly time scales is essential for the development of the two different radiative-turbulent circulation states. As shown by Stramler et al. (2011) the cold and warm circulation anomalies connected with these radiative-turbulent states often persist for days to weeks.

20. On page 11870, LN 6 we introduced the additional sentences: Fig. 12 shows that the wind-scaled heat flux has an almost linear dependence to the vertical temperature difference, indicating a nearly single-valued drag coefficient for heat  $Ch$ . The two circulation states are in the mean connected with either high pressure or low pressure

C5867

systems. Arctic clouds are very often associated with higher near-surface temperatures, but warmer air mass advection and stronger winds contribute to near-surface warming. Under very stable conditions the warm-air advection connected to cyclone passages could reduce the vertical stratification and might result in increased surface sensible heat flux. This changes the surface energy budget and the surface temperature and the outgoing long wave radiation which again impacts on the vertical stability. At the same time the wind changes due to cyclone passages could impact on the wind speeds in the boundary layer and impact on downward turbulent mixing which impact on the stratification. The relations shown in Fig. 12 reflect these conditions with respect to both wind and temperature and show a more pronounced nonlinear variation of Ch for more stable stratification.

The computation of the sensible heat fluxes is described in the Supplementary Fig. Fluxes.

The intermittent turbulence which is visible in Fig. 12 shows differences between the Ch dependence for the two net LW states. For the high pressure state this dependence is more nonlinear. The transitions from strongly stable stratified PBL to well mixed convective PBL and intermittent turbulence over the Arctic Ocean are either due to cyclone effects or ice cracks and open leads due to surface heterogeneities and couldn't be described by the RCM simulations, where a constant sea ice thickness has been assumed.

21. On page 11871, L16 we changed the sentences to: Significant temperature differences between observations and the simulations occur near the surface due to biases in the ABL vertical mixing parameterization, in the treatment of surface processes, sea ice thickness and cloud cover. Additionally the partitioning between stable and near-neutral conditions in the winter ABL in the model simulations could be erroneous.

22. On page 11871, L25 we changed the sentences: HIRHAM simulates too many elevated inversions compared to the NP-35 data, which could be partly connected with

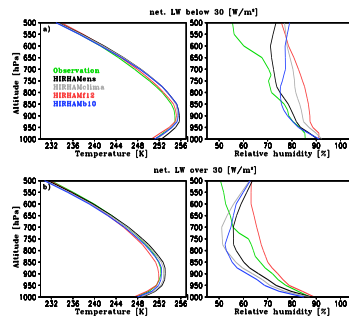
C5868

the poor simulations of vertical cloud layers. The energy budget at the surface and the whole ABL structure are strongly dependent on cloud-radiation processes, but the HIRHAM cloud simulations are biased and no cloud measurements have been carried out on NP-35.

---

Interactive comment on Atmos. Chem. Phys. Discuss., 14, 11855, 2014.

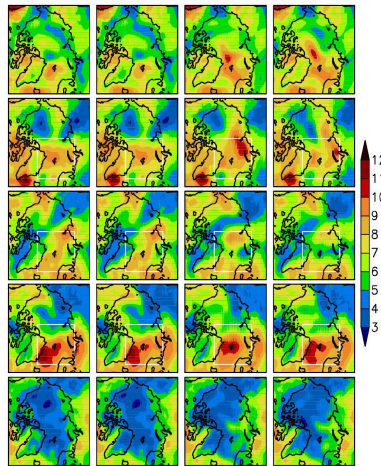
C5869



New Fig. 10 b. Vertical temperature (K) and relative humidity (%) profiles for a) net LW circulation state below  $30 \text{ Wm}^{-2}$  and b) net LW circulation state above  $30 \text{ Wm}^{-2}$  averaged over NDJFM.

Fig. 1.

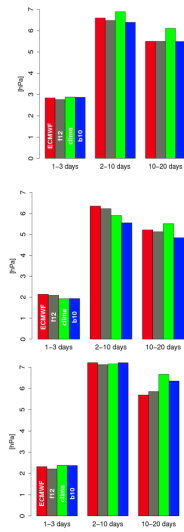
C5870



New Fig. 14. Pan-Arctic distribution of baroclinic-scale variability on time scales from 2–10 days expressed as filtered temporal standard deviation of 6 hourly mean sea level pressure (hPa) for November 2007 (upper row) until March 2008 (lower row) and December, January and February in between. From left to right ECMWF operational analyses, HIRHAM f12 simulations, HIRHAM clima simulations with  $b = 5$ , and HIRHAM b10 with  $b = 10$ .

Fig. 2.

C5871



**New Fig. 16.** Area mean (rectangle indicated by white lines in new Figs. 13-15) of the synoptic and planetary-scale variability on time scales 1-3 days, 2-10 days and 10-20 days for December 2007 (top), January (middle) and February 2008 (bottom). The results are based on filtered standard deviation of 6 hourly mean sea level pressure (hPa). Red column-ECMWF, Grey column-HIRHAM H12, Green column-HIRHAM clima with b5, Blue column-HIRHAM b10.

**Fig. 3.**

C5872

The turbulent sensible heat fluxes have been calculated with the following algorithm, based on the parameterization of Zilitinkevich (1970). Sensible heat fluxes H are calculated very similar to HIRHAM as:

$$H = -T_a c_p \rho U_s$$

U<sub>s</sub> is the wind speed scale, T<sub>a</sub> the temperature scale, ρ air density, c<sub>p</sub> specific heat capacity, κ the Karman constant. The gradients for stable conditions are based on Monin-Obukhov similarity theory, similar to the used model parameterization.

$$\Delta U = \frac{U_s}{\kappa} \left( \ln \frac{z}{z_0} + \beta \frac{z_0 - z_0}{L} \right)$$

$$\Delta T = T_s \left( \ln \frac{z}{z_0} + \beta \frac{z_0 - z_0}{L} \right)$$

L describes the Monin-Obukhov length, z<sub>a</sub>=2m for air temperature and wind speed, z<sub>w</sub>=10m for wind speed, and z<sub>t</sub>=8m for air temperature. ΔU=U<sub>s</sub>-U<sub>0</sub>, the wind speed gradient, ΔT=T<sub>s</sub>-T<sub>0</sub>, the temperature gradient, β=5 and z<sub>0</sub> is the roughness parameter.

**Fig. 4.**

C5873